2022 19th International Conference on Ubiquitous Robots (UR)
July 4-6, 2022. Ramada Plaza Jeju, Jeju, Korea

2022 19th International Conference on Ubiquitous Robots (UR) | 978-1-6654-8253-0/22/$31.00 ©2022 IEEE | DOI: 10.1109/UR55393.2022.9826270

Estimation of Cylinders parameters from point clouds using Least Square Best Fit Method*

In-Gyu Park, Jihyun Park, Hyojun Lee, Jeong-Woo Park, Hyogon Kim, Jeong-Hwan Hwang, Jong-Chan Kim, Kyoungseok Noh, Sung-Jo Yun and Youngho Choi

Abstract—**this paper relates to an algorithm for estimating shape parameters through Least Square Best Fit Cylinder from point cloud data. What is proposed in this paper is to perform least square best fit circle at the same time to obtain information on the start and or end of the cylinder. The reason is that the cylinder shape parameters do not provide accurate starting point information, and the end is not always perpendicular to the cylinder. In order to verify the usefulness of the determined cylinder shape parameters, it is applied to the 3 Dimensional ellipse cutting process of the adjustment pipe. As a result, it precisely calculates the shape parameters of the cylinder and shows that the cylinder's 3 dimensional ellipse cutting operating is precisely performed by using this information.**

I. Introduction

Recently, robots and automation systems have been applied in various industrial fields. For example, bin-picking technology that applies image processing technology of objects with various shapes has developed a lot and is being applied to the fields [1]. However, the cylinder shape is difficult to pick with a simple gripper. So the gripper must grasp accurately. To solve this problem, there have been many studies of using a laser sensor to grasp the shape, position and orientation of a cylindrical objects and then precisely grasping it with a robot gripper [2]. In addition, to improve the robot shaft-in-hole assembly operation beyond the force-controlled coarse assembly method, which is the traditional cylindrical-shaped robot assembly method, 3D vision is used to estimate the object pose combined with admittance control to improve the hole axial position. The work efficiency was improved by estimating and assembly [3]. As a method of fitting data with many outliers, optimized fitting methods that accurately estimate the inlier using the RANSAC (RANdom Sample Consensus) algorithm are used. These methods identify the object containing the optimal inlier and improve the precision of shape information recognition by using the least-square method for accurate shape fitting [4, 5].

In spite of these many papers, the simultaneous study of the cylinder shape and the cylinder end shape and direction has not been identified. In this paper, the least square best fit method was used for the recognition of the cylindrical end as well as the cylindrical object [6].

Recently, many studies have been conducted to find the shape, position, and orientation of the cylinder using point cloud data, which is the shape data of an object measured with a 3D scan or 3D camera [7]. As an example of that, as shown in Fig. 1, the robot system is trying to be applied to the manufacturing process such as adjustment pipe, which is usually an ellipse rather than a circle because the end of the cylinder is inclined [8]. In this process, the shape point cloud information is created by scanning the pipe to be manufactured with a 3D scanner, and a 3D CAD model is created. Using this CAD information, the robot and automation system are driven to enable precise cutting and assembly of pipes.

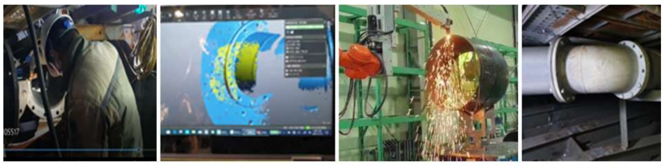

(a) Pipe Scanning (b) 3D Modeling (c) Manufacturing using Robot and Automation (c) Field Installation

Figure 1. Manufacturing of Adjustment Pipe using 3D Scan and Cutting Robot

As another recent example, the automation of the pier assembly process using a robot system at a construction site is being studied [9~11]. Figure 2 shows a concept design of an unmanned pier column construction system combined with an Auto-Climbing form System (ACS), which increases construction efficiency by automatically raising the formwork installation and dismantling, and a robot automation system. As shown in Figure 3, the process sequence of the pier column unmanned construction system is based on the 1st rebar mesh and pier foundation, followed by the 1st rebar mesh and then the 2nd rebar mesh crane to be assembled, and the process of assembling two rebar mesh using three robots arranged at 120 degrees is repeated up to the designed height. In this process, for accurate assembly work using a robot, it is necessary to accurately grasp the position and posture of the rebar mesh and the shape information of the end of the rebar mesh. However, the rebar mesh, which is a heavy object, is deformed by an unbalanced load during movement and is tilted in an arbitrary direction because it is hung on a crane, so there is a fear that an error occurs when assembling using a robot, making it impossible to assemble. In order for this assembly operation to be successful, it is necessary to accurately determine the position and direction of the rebar mesh moved by the crane. In order to solve this problem, the Least Square Best Fit method is applied to the cloud point data obtained by using a 3D camera.

* The research was conducted with the support of the "National R&D Project for Smart Construction Technology No.20SMIP-A158708-02)" funded by the Korea Agency for Infrastructure Technology Advancement under the Ministry of Land, Infrastructure and Transport, and managed by the Korea Expressway Corporation.

In-Gyu Park, Jinyun Park, Hyojun Lee, Jeong-Woo Park, Hyogon Kim, Jeong-Hwan Hwang, Jong-Chan Kim, Kyoungseok Noh, Sun-Jo Yun, and Youngho Choi are with the Korea Institute of Robotics & Technology Convergence(KIRO), Jigok-Ro 39, Nam-Gu, Pohang, Gyeongbuk, 37666, Kore (corresponding author to provide e-mails: igpark, jhpark87, ehyojun, idealcreator, hgkim, hwangjh, jc.kim, ksno, yunsj and rockboy@ kiro.re.kr).

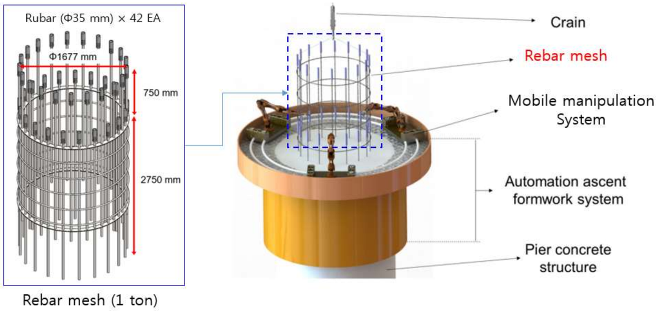

Figure 2. Concept design of pier column unmanned construction system combining ACS and robot system

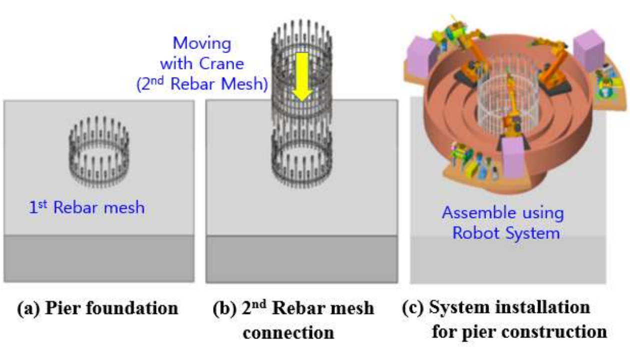

Figure 3. Rebar mesh pier column assembly process using robot technology

Section 2 of this paper introduces the least square best fit method for estimating shape parameters using point cloud data of an object having a cylinder shape. In addition, we introduce the best fitting algorithm for circles to estimate the shape information parameters at the end or start of the cylinder [3]. Section 3 introduces a simulation model to evaluate the usefulness of the introduced least square method. The model is an adjustment pope cutting process in which the start and end of the cylinder have an ellipse rather than a circle. Section 4, the introduced least square best fitting algorithm is verified through simulation. Section 5, summarizes the conclusions of this paper.

II. Least Square Best Fit Method

This chapter introduces the least square best fit method, which derives the parameters that can recognize the object by using the point cloud data, which is the 3D scan result of the object having the cylinder shape. An algorithm for estimating the shape using point cloud data outside the cylinder is introduced, followed by an algorithm for estimating the shape of the circle at the end of the cylinder, the circle estimation algorithm. The reason for estimating the circle is that many cylinder type objects in the industrial field have an ellipse shaped end rather than a circle, so the information on the end of cylinder must be accurately checked.

A. Least Squares Best Fit Cylinder

It is assumed that point m (x_i, y_i, z_i) exists in the cylinder. where m ≥ 5. A cylinder can be expressed by parameterizing a point on the axis (x_0, y_0, z_0), a vector pointing to the long axis, that is, the direction cosine (u_x, u_y, u_z), and radius r.

For any point (x_i, y_i, z_i) to lie on the surface of the cylinder, the vector $(\vec{r_i} - \vec{r_0})$ from the point on the axis (x_0, y_0, z_0) on the axis to any point (x_i, y_i, z_i) on the surface of the cylinder is the direction cosine vector $\vec{n} = [u_x, u_y, u_z]^T$ should have an orthogonal relationship to Equation (1).

$$\vec{n} \times (\vec{r_i} - \vec{r_0}) = 0 \tag{1}$$

The magnitude of the vector that satisfies this condition is the radius R of the cylinder. From the relation between the magnitude vector of the cylinder and the direction cosine vector, a polynomial such as Equation (2) is obtained.

$$a_1y^2 + a_2z^2 + a_3xy + a_4xz + a_5yz + a_6x + a_7y + a_8z + a_9 = -x^2 \tag{2}$$

Equation (2) is expressed as a linear system as equation (3).

$$\begin{bmatrix} y_1^2 & z_1^2 & x_1y_1 & x_1z_1 & y_1z_1 & x_1 & y_1 & z_1 & 1 \\ y_2^2 & z_2^2 & x_2y_2 & x_2z_2 & y_2z_2 & x_2 & y_1 & z_1 & 1 \\ \vdots & \vdots & \vdots & \vdots & \vdots & \vdots & \vdots & \vdots & \vdots \\ y_n^2 & z_n^2 & x_ny_n & x_nz_n & y_nz_n & x_n & y_n & z_n & 1 \end{bmatrix} \begin{pmatrix} a_1 \\ a_2 \\ a_3 \\ a_4 \\ a_5 \\ a_6 \\ a_7 \\ a_8 \\ a_9 \end{pmatrix} = \begin{bmatrix} -x_1^2 \\ -x_2^2 \\ \vdots \\ -x_n^2 \end{bmatrix} \tag{3}$$

This expression is in the form of the normal equation $A^TAP = A^TB$, and the solution to P can be solved as in Equation (4).

$$P = (A^TA)^{-1}A^TB \tag{4}$$

Using the geometric relationship of equation (3), it can be summarized as follows.

- if $|a_3|, |a_4|$ *and* $|a_5|$ converge to 0, and a_1 is closed to 1, it means $[u_x, u_y, u_z]^T = [0,0,1]^T$, and if a_2 is close to 1, it means $[u_x, u_y, u_z]^T = [0,1,0]^T$.
- Otherrwise, each element is multiplied by $k = 2/(k + a_1 + a_2)$. Then the variables can be expressed as equation (5).

$$A = k, B = ka_1, C = ka_2, \cdots, J = ka_9 \tag{5}$$

Where A and B are close to 1

$$\bar{u}_z = \sqrt{1 - C},\ \bar{u}_x = \frac{E}{-2\bar{u}_z},\ \bar{u}_y = \frac{F}{-2\bar{u}_z} \tag{6}$$

If A is close to 1 then B is not close to 1

$$\bar{u}_y = \sqrt{1 - B},\ \bar{u}_x = \frac{D}{-2\bar{u}_y},\ \bar{u}_z = \frac{F}{-2\bar{u}_y} \tag{7}$$

If A is not close to 1

$$\bar{u}_x = \sqrt{1 - A},\ \bar{u}_y = \frac{D}{-2\bar{u}_x},\ \bar{u}_z = \frac{F}{-2\bar{u}_x} \tag{8}$$

The direction $[\bar{u}_x, \bar{u}_y, \bar{u}_z]^T$ is normalized to get the direction $[u_x, u_y, u_z]^T$.

Knowing the direction vector $[u_x, u_y, u_z]^T$, we construct a linear system as in equation (9) to compute an initial estimate for $[x_0, y_0, z_0]^T$ using the coefficients a_6, a_7, a_8 and the definition of the equation $u_xx_0 + u_yy_0 + u_zz_0 = 0$.

$$\begin{bmatrix} -2(u_y^2 + u_z^2) & 2u_xu_y & 2u_xu_z \\ 2u_xu_y & -2(u_x^2 + u_z^2) & 2u_bu_z \\ 2u_xu_z & 2u_yu_z & -2(u_x^2 + u_y^2) \\ u_x & u_y & u_z \end{bmatrix} \begin{pmatrix} x_0 \\ y_0 \\ z_0 \end{pmatrix} = \begin{bmatrix} a_6 \\ a_7 \\ a_8 \\ 0 \end{bmatrix} \tag{9}$$

Equation (9) can estimate the initial position value in the same way as equation (4). The radius R is estimated at an initial value by equation (10), which is the result of arranging the coefficient a_9 term.

$$R^2 = (u_y^2 + u_z^2)x_0^2 + (u_x^2 + u_z^2)y_0^2 + (u_x^2 + u_y^2)z_0^2 - 2u_y u_z y_0 z_0 - 2u_y u_z y_0 z_0 - 2u_y u_z y_0 z_0 - a_9 \quad (10)$$

The process of obtaining an optimal parameter estimate using the initial estimate information obtained above follows the procedure below.

Step 1. Translation of origin

The data is copied and translated so that the point on the axis is at the center of the point

$$[x_i, y_i, z_i]^T = [x_i, y_i, z_i]^T - [x_0, y_0, z_0]^T \quad (10)$$

Step 2. Rotational translation is performed with a rotation matrix U that rotates $[u_x, u_y, u_z]^T$ to a point on the z-axis.

$$\begin{bmatrix} x_i \\ y_i \\ z_i \end{bmatrix} = \mathrm{U} \begin{bmatrix} x_i \\ y_i \\ z_i \end{bmatrix} \quad (11)$$

Where U is

$$\mathrm{U} = \begin{bmatrix} c_2 & 0 & s_2 \\ 0 & 1 & 0 \\ -s_2 & 0 & c_2 \end{bmatrix} \begin{bmatrix} 1 & 0 & 0 \\ 0 & c_1 & -s_1 \\ 0 & s_1 & c_1 \end{bmatrix} \quad (12)$$

When $[u_x, u_y, u_z]^T = [1,0,0]^T$, $s_1 = 0, c_1 = 1, s_2 = -1, c_2 = 0$.

Otherwise,

$$c_1 = \frac{u_z}{\sqrt{u_y^2 + u_z^2}}, \quad s_1 = \frac{u_y}{\sqrt{u_y^2 + u_z^2}},$$

$$c_2 = \frac{u_z c_1 - u_y s_1}{\sqrt{u_x^2 + (u_z c_1 - u_y s_1)^2}}, \; s_2 = \frac{-u_x}{\sqrt{u_x^2 + (u_z c_1 - u_y s_1)^2}} \quad (13)$$

Step 3. Construct and solve a linear system

$$J \begin{pmatrix} p_{x0} \\ p_{y0} \\ p_a \\ p_b \\ p_r \end{pmatrix} = -d \quad (14)$$

The Jacobian matrix J is the same as equation (15).

$$J = \begin{bmatrix} -x_1/r_1 & -y_1/r_1 & -x_1 z_1/r_1 & -y_1 z_1/r_1 & -1 \\ -x_2/r_2 & -y_2/r_2 & -x_2 z_2/r_2 & -y_2 z_2/r_2 & -1 \\ \vdots & \vdots & \vdots & \vdots & \vdots \\ -x_n/r_n & -y_n/r_n & -x_n z_n/r_n & -y_n z_n/r_n & -1 \end{bmatrix} \quad (15)$$

The distance from the point$[x_i, y_i, z_i]^T$ to the cylinder is the same as equation (16).

$$\mathrm{d} = r_i - r \quad (16)$$

Where

$$r_i = \frac{\sqrt{l_i^2 + m_i^2 + n_i^2}}{\sqrt{u_x^2 + u_y^2 + u_z^2}} \quad (17)$$

$$l_i = u_z(y_i - y_0) - u_y(z_i - z_0)$$

$$m_i = u_x(z_i - z_0) - u_z(x_i - x_0)$$

$$n_i = u_y(x_i - x_0) - u_x(y_i - y_0)$$

Step 4. Update parameter estimates

$$\begin{pmatrix} x_0 \\ y_0 \\ z_0 \end{pmatrix} = \begin{pmatrix} x_0 \\ y_0 \\ z_0 \end{pmatrix} + U^T \begin{pmatrix} p_{x0} \\ p_{y0} \\ -p_{x0}p_a - p_{y0}p_b \end{pmatrix}$$

$$\begin{pmatrix} u_x \\ u_y \\ u_z \end{pmatrix} = U^T \begin{pmatrix} p_a \\ p_b \\ 1 \end{pmatrix} \quad (18)$$

$$r = r + p_r$$

Repeat until the estimate update value is small enough.

B. Least Squares Best Fit Circle

We want to fit a circle to m points (x_i, y_i, z_i) with $\mathrm{m} \geq 3$ in 3D space. A circle can be parameterized with a center point (x_0, y_0, z_0), a radius r, and a vector (u_x, u_y, u_z) perpendicular to the plane containing the circle. The distance from any point to a 3 Dimensional circle can be expressed by equation (19)

$$d_i^2 = e_i^2 + f_i^2 \quad (19)$$

Where,

$$e_i = \sqrt{(x_i - x_0)^2 + (y_i - y_0)^2} - r \quad (20)$$

$$f_i = z_i \quad (21)$$

In equation (19), d_i^2 is itself the sum of two squares, and for this reason, it is modeled as minimizing the element fitting problem.

For the initial estimation of the parameters, a plane is fitted to the data points to obtain an estimate of the centroid $[\bar{x}, \bar{y}, \bar{z}]^T$ and $[u_x, u_y, u_z]^T$. Then, the data points are translated so that $[\bar{x}, \bar{y}, \bar{z}]^T$ becomes $[0,0,0]^T$, and $[u_x, u_y, u_z]^T$ is converted to a point on the z-axis. Now, in the state transformed into a 2-dimensional problem, we find the optimal circle for the x and y coordinates. An initial estimate is obtained as in equation (22).

$$\begin{bmatrix} x_0 \\ y_0 \\ z_0 \end{bmatrix} = \begin{bmatrix} \bar{x} \\ \bar{y} \\ \bar{z} \end{bmatrix} + U^T \begin{bmatrix} x_i \\ y_i \\ z_i \end{bmatrix} \quad (22)$$

The algorithm for minimizing equation (19) above proceeds according to the following steps.

Step 1. Copy and translate the data so that the centroid estimate is at the origin.

$$[x_i, y_i, z_i]^T = [x_i, y_i, z_i]^T - [x_0, y_0, z_0]^T \quad (23)$$

Step 2. A rotational translation is performed with a rotation matrix U that rotates $[u_x, u_y, u_z]^T$ to a point on the z-axis.

$$\begin{bmatrix} x_i \\ y_i \\ z_i \end{bmatrix} = \mathrm{U} \begin{bmatrix} x_i \\ y_i \\ z_i \end{bmatrix} \quad (24)$$

Step 3. Construct and solve a linear system

$$\begin{bmatrix} J_e \\ J_f \end{bmatrix} \begin{pmatrix} p_{x0} \\ p_{y0} \\ p_{z0} \\ p_a \\ p_b \\ p_r \end{pmatrix} = \begin{bmatrix} -e \\ -f \end{bmatrix} \quad (25)$$

Jacobian is the same as equation (26)

$$\begin{bmatrix} J_e \\ J_f \end{bmatrix} = \begin{bmatrix} -x_i/r_i & -y_i/r_i & 0 & -x_i z_i/r_i & -y_i z_i/r_i & -1 \\ 0 & 0 & -1 & x_i & y_i & 0 \end{bmatrix} \quad (26)$$

Step 4. Update parameter estimates

$$\begin{pmatrix} x_0 \\ y_0 \\ z_0 \end{pmatrix} = \begin{pmatrix} x_0 \\ y_0 \\ z_0 \end{pmatrix} + U^T \begin{pmatrix} p_{x0} \\ p_{y0} \\ p_{z0} \end{pmatrix}$$

$$\begin{pmatrix} u_x \\ u_y \\ u_z \end{pmatrix} = U^T \begin{pmatrix} p_a \\ p_b \\ 1 \end{pmatrix} \quad (27)$$

$$r = r + p_r$$

Repeat until the estimate update value is small enough.

III. SIMULATION

In order to verify the usefulness of the cylinder estimation algorithm developed in the previous Section, simulation verification is performed on the 3D cutting process of the adjustment pipe having an arbitrary position and orientation. The simulation model was constructed and analyzed with DAFUL, a dynamics analysis program, and the results were verified.

A. SIMULATION MODEL

The robot system is configured as shown in Figure 4, and the plasma cutting robot arm is attached at the end of the industrial robot. A plasma cutting module is installed at the end of this robot arm, and it is used to cut pipes [8]. A 3 D scanner or 3D camera module can be used as a sensor system for recognizing a pipe. The pipe shape point cloud data information obtained from these sensor system is utilized. The adjustment pipe applied to the 3 dimensional cutting test has a diameter of 500A and a length of 300 mm.

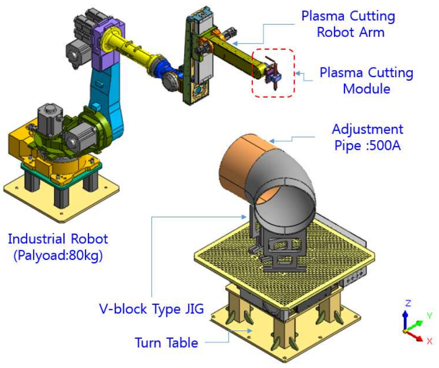

Figure 4. Plasma cutting robot system used in simulation

The coordinate frame of the robot for plasma cutting is shown in Figure 4. Based on the industrial robot coordinate frame $\{O_R - XYZ\}$, there is the plasma cutting robot coordinate system $\{O_P - XYZ\}$ attached to the end of the robot, and this coordinate system is used together as the coordinate $\{O_D - XYZ\}$ to which the digitizer or camera sensor is attached. From the obtained pipe position and orientation $\{O_{PC} - XYZ\}$ data, move to the position $\{O_W - XYZ\}$ of the plasma cutting robot for pipe cutting, then perform the cutting process.

In figure 6, based on the coordinate system $\{O_{PC} - XYZ\}$ of the pipe identified through measurement, the cut length d_C, which is the cutting parameter, and 3 dimensional elliptical coordinate system $\{O_C - XYZ\}$ translated by the cutting angle θ_y are placed.

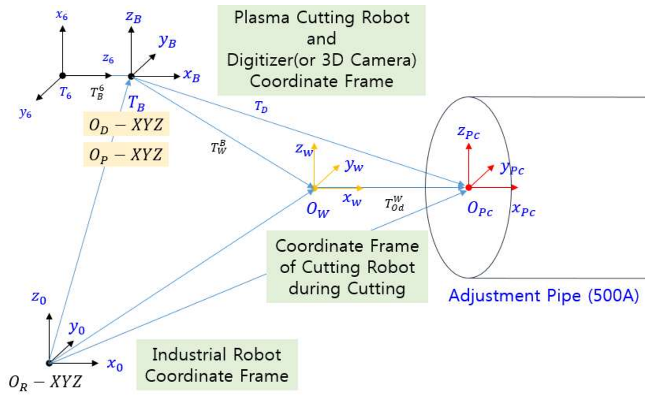

Figure 5. Coordinate frame of plasma cutting robot system

The information of cloud point data for estimating adjustment pipe to be used in this simulation is shown in figure 7. It was obtained using CAD data, and disturbance was added to more than 1/3 of the data in consideration of the measurement error. For the least square best fit cylinder, a total of 84 data were obtained by collecting the pipe surface data 12 at a time at 20 mm intervals, and 12 data among them were used for cylinder estimation (blue diamond). Then, in order to know the shape information of the pipe end, a total of 10 data were measured at the end of the adjustment pipe, and 5 data among them were used for least square best fit circle (red circle).

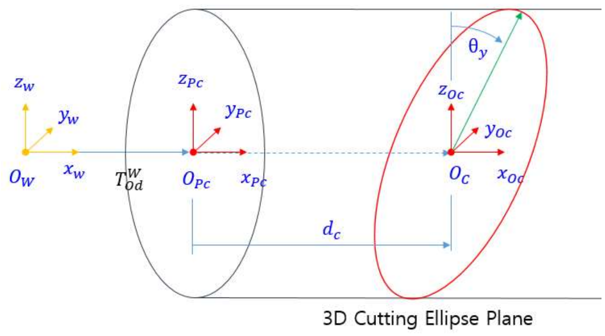

Figure 6. Coordinates and cutting parameters of pipe for 3D ellipse cutting

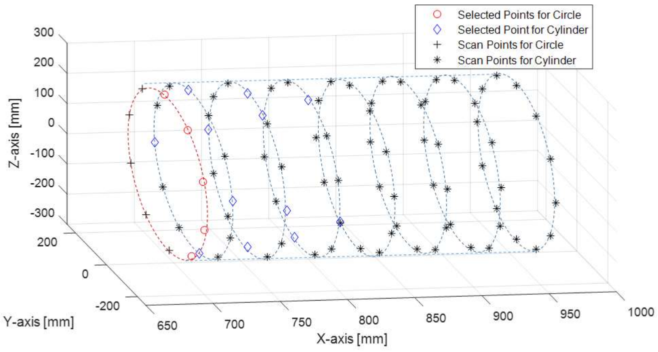

Figure 7. Scan data of a cylinder using 3D scanner (wrt Scanner coordinate frame)

B. RESULT OF SIMULATION

Table 1 shows the results of shape recognition parameter optimization through least square best fit of an adjustment pie having a cylinder shape. In order to understand the usefulness of the estimate, the CAD model value and the estimated value were compared.

Least square best fit cylinder shape estimation results are as follows. In the case of cylinder shape estimation, it can be seen that the direction cosine value matches with a very precisely matched with the CAD modeling value, and also the Radius value. However, it was found that the value of Initial position was recognized at a point close to 0, different from the value of CAD. So, additional estimation of the circle at the end of the cylinder was performed, which is not only to recognize the end of the cylinder, but to identify the inclined shape of the end of the cylinder. The result shows that the shape parameters of the circle, initial position, direction cosine, and radius are precisely estimated.

TABLE 1. The Results of Least Square Best-Fit Cylinder

Division		Target Value (CAD)	Best-fitted Value (Simulation)
Circle	Initial Position	694.998,0,0	694.981,2.4e-05,2.4e-05
	Direction Cosine	1,0,0	1, -2.26e-05,1.24e-05
	Radius	250.45	250.448
Cylinder	Initial Position	694.998,0,0	-
	Direction Cosine	1,0,0	1,-1.61e-13,-1.81e-13
	Radius	254.4	254.4

Figure 8 shows the motion simulation results for plasma cutting operation using DAFUL. The blue solid line is the elliptical trajectory of the 3 dimensional cutting surface of the adjustment pipe, and the red solid line is the comparison of the motion trajectory of the tip of the plasma cutting module of the plasma cutting robot arm.

As a result, it can be seen that the two trajectories coincide, so that the tip traces the 3 dimensional elliptical trajectory well. The maximum error is shown in figure 9. As a result, it was confirmed that the y-axis and z-axis are each within the maximum range of ±0.36 mm, and in the case of the x-axis, it is table within the maximum ±0.002 mm.

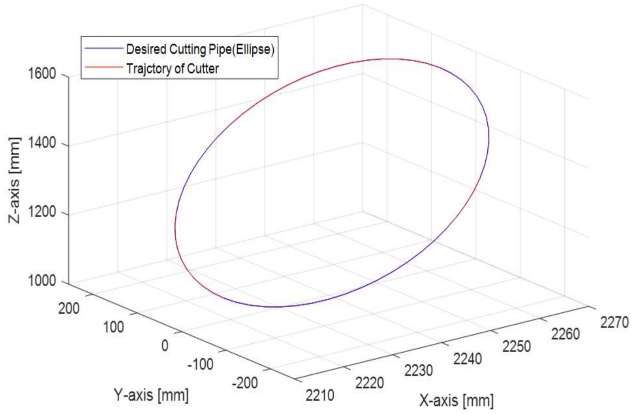

Figure 8. Comparison of results of 3 dimensional elliptical cut of cylinder

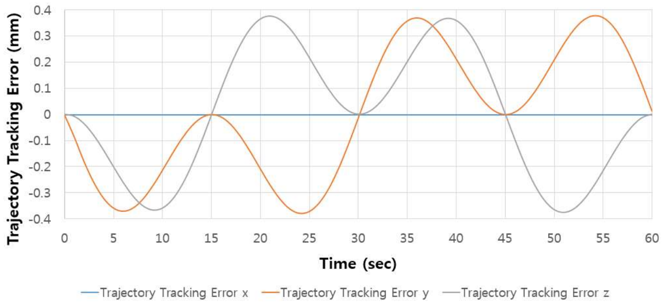

Figure 9. Error for each direction when cutting

IV. CONCLUSION

In this paper, an estimation algorithm for cylindrical objects, which is difficult for automated production work due to the inability to grasp the size and direction, is introduced and verified through simulation. In general, for recognizing such an object, a 3D scanner or 3D camera is used to recognize the object and obtain point cloud data. However, in this paper, point cloud information is obtained from CAD data, and the perturbation value is added to the 1/3 data by considering the measurement error in the value. By selecting all or part of the obtained data, the least square best fit method was applied to estimate the shape parameters of the cylinder. The results are summarized as follows.

- In order to recognize the pipe lying in any cylinder shape, position and direction, the least square best fit method was introduced.
- To recognize the pipe shape, two step estimation analysis was performed. First, the estimation algorithm for the cylinder is performed. Then, we propose a method of continuously performing an estimation algorithm for a circle to determine the shape information of the cylinder end. As a result, it is possible to estimate the cylinder end information and products whose ends are not cut vertically.
- In order to verify the algorithm, a robot automation system that can perform cutting work by applying it to the adjustment pipe was introduced and the procedure was explained.

- The point cloud data was extracted from the CAD model, and more than 1/3 of the extracted values were perturbed and used to verify the cylinder shape parameter estimation algorithm. As a result, the cylinder matched with the CAD model, and it was confirmed that the shape parameters were accurately estimated within the error range of 2.5e-05 for the circle, which is the end of the pipe.
- Based on this estimated information, as a result of simulation verification using DAFUL, it was confirmed that the tracking was well within ±0.36 mm.

REFERENCES

[1] Udaya Wijenayake, Sung-In Choi, and Soon-Yong Park, "Stereo Vision-Based 3D Pose Estimation of Product Labels for Bin Picking," J of ICROS, vol. 22(1), pp. 8–16, 2016.

[2] Jeong, Kyuwon, "Pose estimation of a Cylindrical Object for an Inspection Robot," *KSMTE*, vol. 12, pp. 8–15, Feb. 2003.

[3] Can Li, Ping Chen, Xin Xu, Xinyu Wang and Aijun Yin, "A Coarse-to-fine method for estimating the axis pose based on 3D point cloud in Robotic cylindrical shaft-in-hole assembly," J of Sensors, vol. 21(12) 4064, pp. 1–20, 2021.

[4] Abdul Nurunnabi, Yukio Sadahiro and Roderik Lindenbergh,"Robust Cylinder Fitting in Three-Dimensional Point Cloud Data," ISSPRS, vol. XLII-1/W1, pp. 63-70, June. 2017.

[5] Trung-Thien Tran, Van-Toan Cao, and Denis Laurendeau,"Efficient CUDA implementation of Multiple Planes Fitting Using RANSAC," JKIICE, vol. 23(4), pp. 388-393, Apr. 2019.

[6] Forbes, Alistair B., Least Squares Best-Fit geometric elements, NPL report April 1989.

[7] Trung-Thien Tran, Van-Toan Cao, and Denis Laurendeau,"Extraction of cylinders and estimation of their parameters from point clouds," Computers & Grapics, vol. 46, pp. 235-357, Feb. 2015.

[8] In-Gyu Park, "Development of 3 Dimensional Precision cutting Robot System using Plasma Cutter for Adjustment Pipe obtained from Shape in the Shipyard," ICCAS 2021, pp. 2077-2082, Oct. 2021.

[9] Taeil Chun, Sang-Won Lee, Sang-Yoon Lee, and Jee-Hwan Ryu, "Design of Manipulator end Effectors for Pier Column Construction," *J of Korea Robotics Society*, vol. 16(3), pp. 207–215, 2021.

[10] Jeong-Woo Park, Kyoung-Seok Noh, Hyo-Gon Kim, Hyo-Jun Lee, Ji-Hyun Park, Jin-Ho Suh, and Young-Ho Chio, "Development of Multiple Manipulation System for Precise Installation of Girder," *J of Power System Engineering*, vol. 25(6), pp. 45–53, Dec. 2021.

[11] Hyo-Gon Kim, Jong-Chen Kim, Jeong-Hwan Hwang, Jeong-Woo Park, Ji-Hyun Park, Jin-Ho Suh and Young-Ho Chio, "Development of a Mobile Manipulation System for Pier Construction," *J of Power System Engineering*, vol. 25(6), pp. 38–44, Dec. 2021.